ATOMIC FORCE MICROSCOPY ANALYSIS OF EFFECT OF RF/DC POWER RATIO ON THE PROPERTIES OF CO-SPUTTERED $Ti_XAl_{1-X}N$ THIN FILMS

Ashwini Kumar Singh*, Neelam Kumari, S. K. Mukherjee & P.K. Barhai
Dept of Applied Physics, BIT, Mesra, Ranchi-835215, Jharkhand, India.

ABSTRACT

$Ti_{1-x}Al_xN$ coatings were deposited using separate Ti and Al targets by reactive RF / DC magnetron co-sputtering on Si and stainless steel substrates. The phase, microstructure, surface roughness and chemical compositions were investigated. The thickness of the coatings were found to be in the range 450 ~ 650nm and possess grain sizes less than 10nm. The roughness of the coatings was found to decrease with increasing sputter power. The compositional analyses of the coatings revealed that with increasing power the ratio of Al to Ti varies. The corrosion behaviour of the films in 3.5% NaCl solution was investigated using electrochemical technique.

Keywords: *$Ti_{1-x}Al_xN$ coatings, reactive RF / DC magnetron co-sputtering, Atomic Force Microscope, power ratio*

1. INTRODUCTION

TiAlN coatings have been attracting more and more attentions since last decade due to their high oxidation resistance (800− 900 °C), high hardness (30-35GPa) and high corrosion resistance [1]. TiAlN coatings are used in cutting tools, especially for dry and high speed machining [2]. TiAlN films significantly increase the tool life and the downtime of the instrument compared to TiN films [3]. Owing to these properties of TiAlN coatings they can be used as high-density complementary metal-oxide-semiconductor (CMOS) memory devices [4], temperature controller for the satellites in the form of heat shield [5] and selective coatings for solar collectors [6-8]. TiAlN films can also be used as bio-implants [9]**.** Properties of the TiAlN coatings are highly dependent on the Al content and phase structure of the coatings [10-12]. The industrial use of TiAlN coatings is in the field of high temperature cutting operations with minimum use of lubricant while machining titanium, aluminum, nickel alloys, stainless steels, alloy steels, Co-Cr-Mo and cast irons [13]. TiAlN coatings are also used to protect dies and molds that are operated at high temperature [14]. Industries need super hard coatings for the hard and tough materials machining. Development of material and its machining needs nitride based films as competitive candidate and TiAlN is one among them [15].

Magnetron sputtering is used, in particular, as it is easy to reproduce the films with similar properties. It can develop thin films on complex shapes with high flexibility of orientation and composition [16]. Position of target and the substrate is responsible for the incoming ion flux direction on the substrate which produces a significant change in the film properties. Even substrate rotation can lead to significant changes in their structure [17]. Because of these advantages reactive magnetron sputtering is one of the most popular technique for deposition of the films on various substrates.

$Ti_{1-x}Al_xN$ coatings were developed using reactive magnetron sputtering system as it does not requires toxic gases for the deposition which makes it environment friendly[13]. It is very simple and low temperature processing is possible. Film characterization involves investigation of surface morphology using SEM, qualitative analysis of elemental composition with the help of EDX. In this paper, the effect of variation of RF/DC power ratio on the structural, morphological and compositional properties of $Ti_{1-x}Al_xN$ coated thin films has been investigated.

The properties of the RF/DC co−sputtered deposited $Ti_{1-x}Al_xN$ films were correlated with the applied power ratio of RF/DC.

2. EXPERIMENTAL

$Ti_{1-x}Al_xN$ thin films were deposited on clean Si and stainless steel (SS) substrates using reactive RF/DC magnetron co-sputtering deposition unit (Vacuum technique pvt. Ltd., Banglore). A schematic diagram of the RF/DC magnetron Sputtering deposition system is shown in Fig 1. Ar gas (99.99%) was used for deposition. The RF/DC magnetron co-sputtering system consists of dual targets, MKS type 247 mass flow controllers, sample holder and view port. Pure Al and Ti target (50 mm diameter, 5 mm thick, 99.99% pure) was mechanically clamped to the magnetron cathode of the sputtering system. 300 W RF power supply was used to power the Al target while The Ti target was powered by a 1 kW DC power supply.
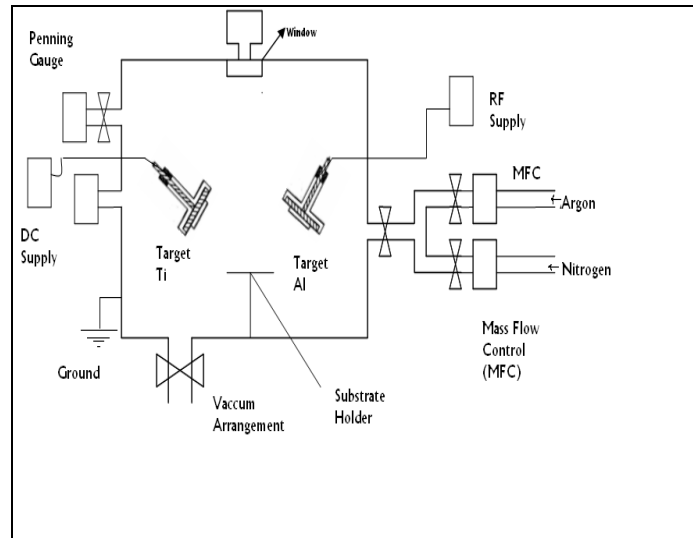
Figure 1.   Schematic Diagram of DC Magnetron Sputtering System.

Silicon substrates of size 10×10 mm^2 and thickness ~ 0.5mm and SS substrates are circular with a diameter of 10 mm diameter and thicknesses ~ 5mm were used for deposition.

The substrates were ultrasonically cleaned for 30 min using isopropyl alcohol and dried at room temperature prior to deposition. Substrates were mounted on the sample holder and a base pressure of ~10^{-6} mbar was obtained. The target surface and the substrates were sputter etched inside the deposition chamber using Ar at 100 W for 20 min to avoid contamination before deposition. After sputter cleaning, Ar: N$_2$ gas flow rate was adjusted to 4:6 ratios and working pressure of ~ 3.5 x 10^{-2} mbar was maintained during deposition. In this way, films were obtained at five different RF/DC power ratios (1.0, 1.2, 1.4, 1.6, 1.8 and 2.0). The deposition conditions and film thicknesses are summarized in Table 1.

Table 1: Power Ratio, composition of Ti, Al and N, Corrosion current and voltage, film thickness for films deposited at different power ratios.

Sample Name	RF (Watt)	DC (Watt)	DC/RF Ratio	N (%)	Al (%)	Ti (%)	E_{corr} (mV)	i_{corr} (μA/cm2)	RMS roughness (nm)	Average roughness (nm)	Film Thickness (nm)
S1	100	100	1	82.89	13.12	3.99	-69.30	8.61	5.25	6.593	450.00± 10
S2	105	125	1.2	63.61	17.31	19.08	-69.76	8.55	4.785	6.125	455.00± 10
S3	110	150	1.4	33.2	26.46	22.01	-50.32	7.59	4.553	5.132	475.00± 10
S4	125	200	1.6	38	30.48	31.52	-50.61	5.86	3.659	4.971	550.00± 10
S5	140	250	1.8	24.35	40.32	35.33	-47.63	3.76	3.824	3.697	581.00± 10
S6	150	300	2	19.37	41.11	39.52	-45.13	1.45	1.98	2.5	650.00± 10
Substrate							-110.6	8.75			

Crystallographic analyses of the deposited films were done by GIXRD (Model: Bruker D8 Advance X-ray diffractometer). The x- rays were produced using a sealed tube and the wavelength of x-ray was 0.154 nm (Cu K-alpha). The x-rays were detected using a fast counting detector based on Silicon strip technology (Bruker LynxEye dtector). For the surface roughness analysis Atomic Force Microscope (AFM NT-MDT, Solver Pro 47) was used. The surface morphology of Ti$_{1-x}$Al$_x$N films were analyzed using SEM (JEOL, JSM−6390LV). Thickness of the films was measured using Ellipsometer (Nano- View Inc., SEMG1000-VIS) with instrumental error of ± 10 nm error bar. Corrosion studies were performed using ECA (CH Instruments, 680B).

3. RESULTS AND DISCUSSION

The x-ray diffraction patterns obtained from the film surface (Fig. 2) shows the formation of polycrystalline films of $Ti_{1-x}Al_xN$. It is sustained by the presence of the cubic TiAlN (100) peak appearing at (21.79) JCPDS Card no: 37-1140 and hexagonal TiAlN (114) peak placed at (68.92) JCPDS Card no: 18-0070. XRD spectra reveals that the coatings with low Al content show small hexagonal (Ti, Al)N phase and major cubic (Ti, Al)N Phase. This might have resulted due to the incorporation of cubic TiN in place of hexagonal AlN phase [18].
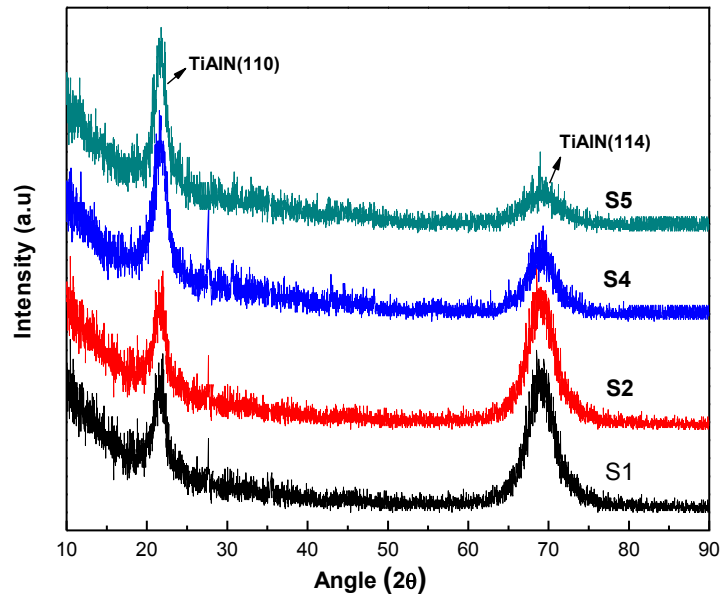
Figure 2.   GIXRD diffraction pattern of deposited films prepared at different RF/DC power ratios.

EDS spectra have prominent peaks of Ti, Al, N and Si in the samples (Fig. 3). The results of the EDS analysis are tabulated in Table 1. Each data is an average of 10 readings taken at 10 different positions. The Si contents were neglected assuming that the Si signals are coming from the substrate and are hence not included in the analysis.
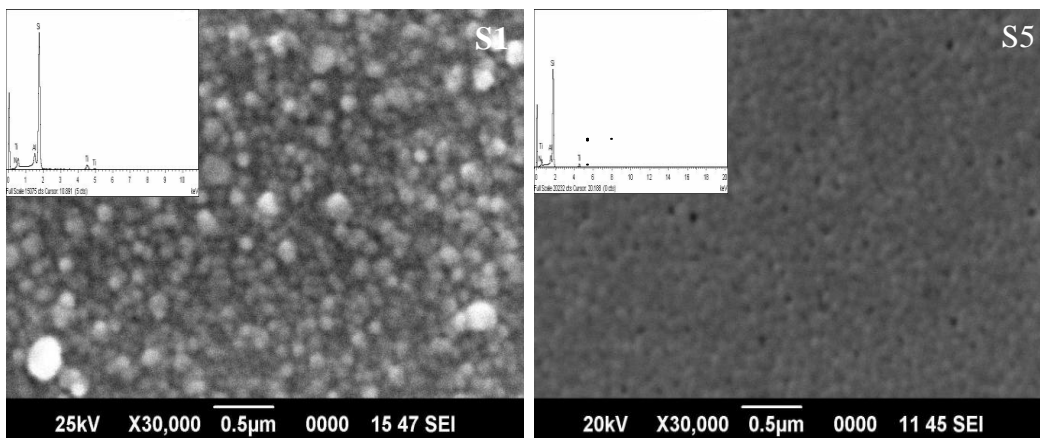

Figure 3. SEM image and EDS spectra of $Ti_{1-x}Al_xN$ thin films deposited at different RF/DC power ratio; S1 and S5.

From the data it is observed that N was reduced from 82.89 to 19.37 wt (%) whereas Ti and Al increased from 13.12 and 3.99 to 41.11 and 39.52 respectively (Fig. 4). SEM images for the higher power ratio shows smooth film surface with smaller grains, whereas for lower power ratio surface is rough and the grains are of larger size (Fig. 3). TiN

phase has been found to be less than AlN phase and hence resulted in denser and compact surface with varying Al/Ti ratio.
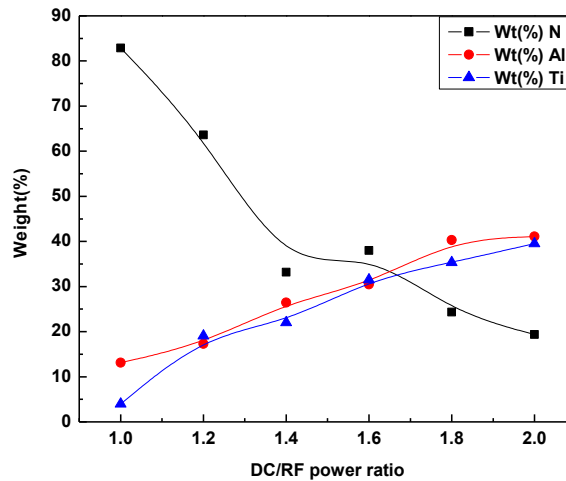

Figure 4. Weight % of N, Al and Ti for different $Ti_{1-x}Al_xN$ thin films.

AFM used for morphological analysis of the coating. The average roughness, grain size and the root mean square (RMS) roughness were obtained for the TiAlN films as a function of power ratio. The average roughness and RMS roughness data were obtained on scanned area of 400 nm X 400 nm where ten different points were used for the calculation of the average value. It was observed that the grain size (Fig. 5), average and the RMS roughness (Fig. 6) have a tendency to decrease as a function of the increased power ratio. The grain size of the thin film grows due to grains nucleation, competitive and stable growth (Fig. 5 S1(c)). Grains of lowest superficial energy incorporate more material and grow on grains with highest superficial energy due to the migration of adatoms between neighboring grains. The surface so obtained was in form of "V" shape [19]. At higher power ratio surface morphology, i.e., "V" shape (Fig. 5 S5(c)); remained the same with small granular structure due to incorporation of more Al atom in the film than Ti (Fig. 5 S1(a)). Coating so obtained was in the form of even repetition of nanosized crystallites [20]. This behavior is probably due to heating of the substrate at higher power ratio. Heating have provided sufficient energy to the adatoms for returning to the plasma and hence the deposition is with relatively less TiN phase [21]. Surface morphology can be better understood by quantitative analysis of the topography in two dimensions as well as three dimensions. The four surface profile parameter namely: amplitude or height, spacing, hybrid and functional or statistical is used for quantitative analysis. Height/amplitude parameter is the principal parameter in surface topography characterization. The average roughness (R_a) and the root mean square roughness (R_q) is the most used amplitude parameters. Equations involved for the height parameters analysis of the three dimensional (3D) topographic surface profile matrix data are [22, 23]:

Arithmetic average height ($\bar{Z}$)

$$\bar{Z}(N,M) = \frac{1}{NM} \sum_{x=1}^{N} \sum_{y=1}^{M} Z(x,y)$$

Average roughness (R_a)

$$R_a(N,M) = \frac{1}{NM} \sum_{x=1}^{N} \sum_{y=1}^{M} (Z(x,y) - \bar{Z}(N,M))$$

Root Mean Square Roughness (RMS) (R_q)

$$R_q(N,M) = \sqrt{\frac{1}{NM} \sum_{x=1}^{N} \sum_{y=1}^{M} (Z(x,y) - \bar{Z}(N,M))^2}$$
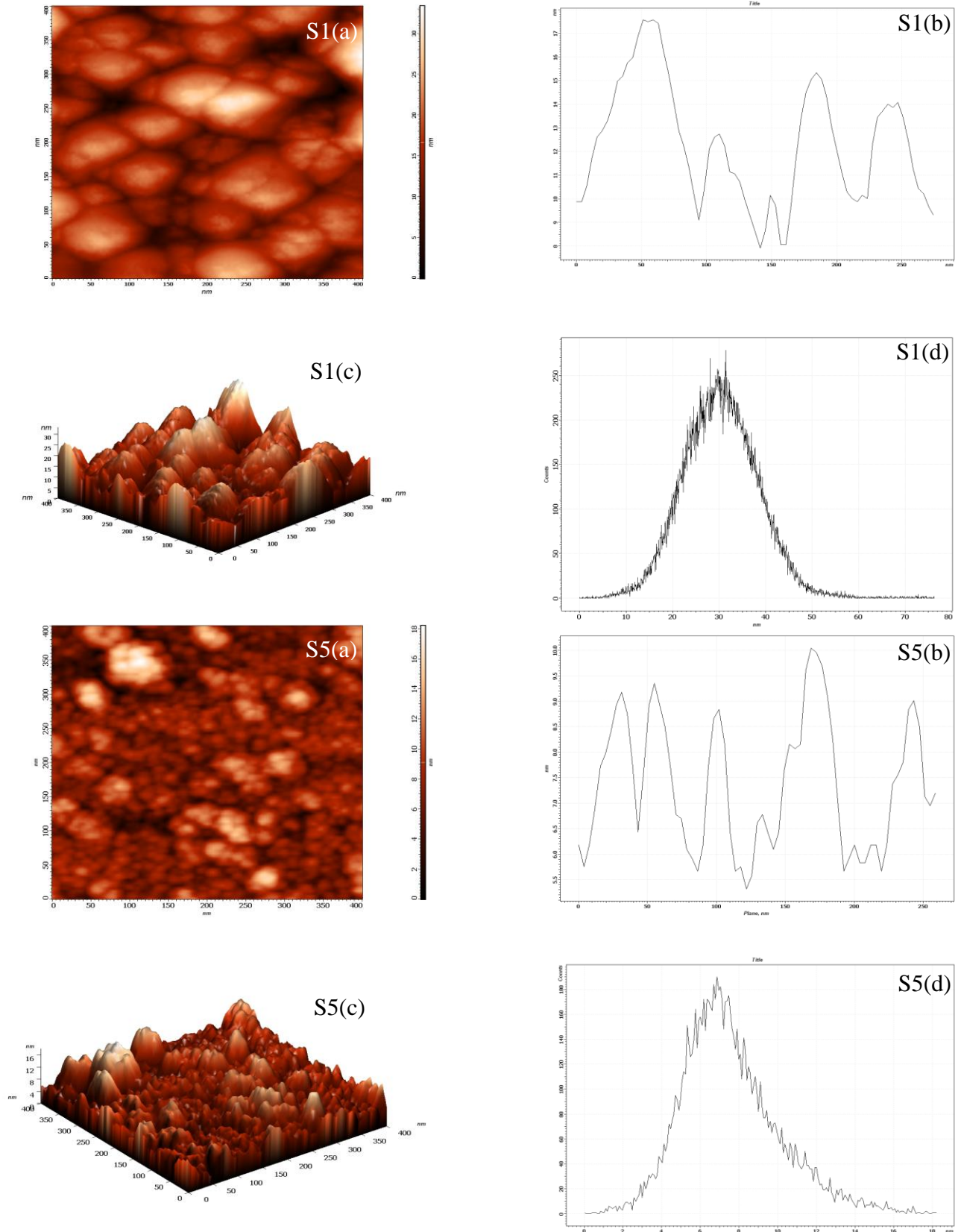
Figure 5. AFM image for surface topography of Ti$_{1-x}$Al$_x$N thin films of S1 and S5; (a) 2 dimensional image, (b) grain size distribution graph, (c) 3 dimensional image and (d) histogram of 400nm scan.

Where:

N-number of data points

M-number of peaks and valleys that needs to be considered

Z-surface height at each data point

$\bar{Z}$-average height of the surface profile

R_a-Average roughness

R_q-Root Mean Square Roughness

The height parameters so obtained is summarized in Table 1. As per the analysis results it is confirmed that average roughness and the RMS roughness of the films reduced from 5.25 nm and 6.54 nm to 1.98 nm and 2.5 nm respectively. Size distribution histogram shows that most of the particles are within 10 to 40 nm and at higher power ratio it reduces below 10 nm. Therefore it can be inferred that with replacement of TiN by AlN and with more incorporation of Al, the films show better smoothness [18].
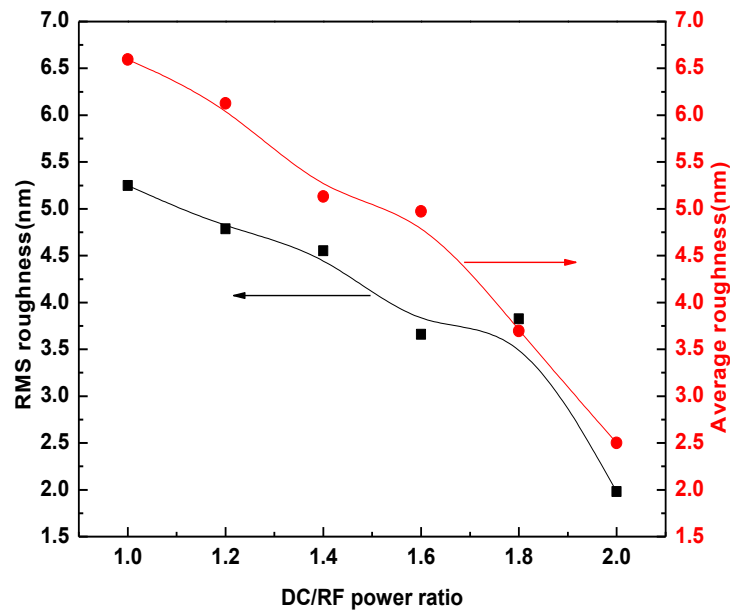

Figure 6. RMS and Average roughness for different Ti$_{1-x}$Al$_x$N thin films.

Corrosion analyses of the films were done both on coated as well as uncoated substrates. The results of corrosion testing for the substrate and the coated film in 3.5% NaCl are shown in Table 1. The corrosion potential of the substrate was about 0.110 V. The corrosion current I$_{corr}$ of substrate was greater than those of Ti$_{1-x}$Al$_x$N coated films. I$_{corr}$ in case of substrate was 8.75µA/cm^2 and with coating on the substrate it reduced gradually to 1.45µA/cm^2 (Fig 7). It shows that Ti$_{1-x}$Al$_x$N coating on substrate at higher power ratio has higher corrosion resistance as suggested by other authors [24].
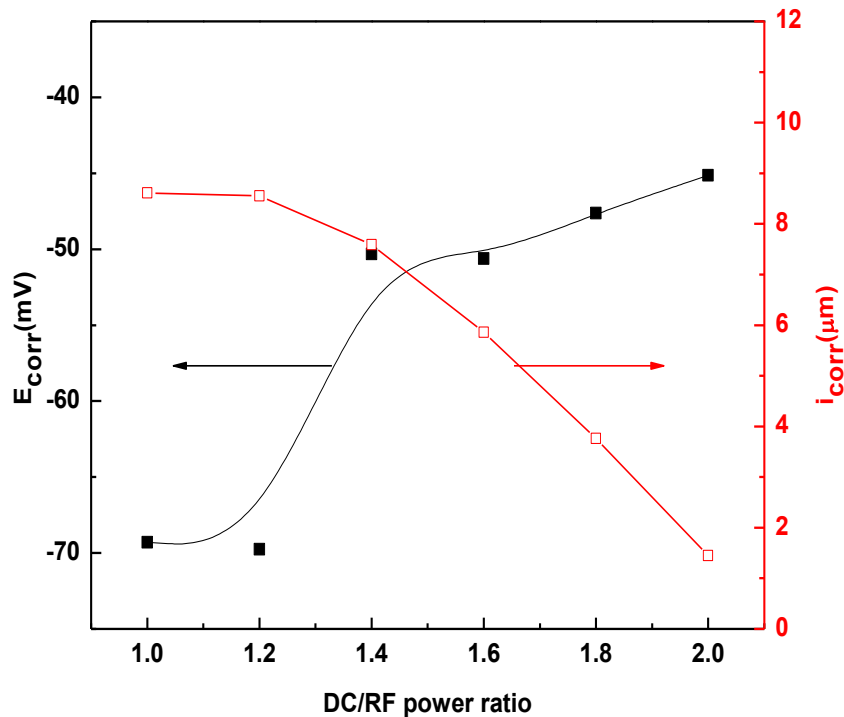
Figure 7. E_{corr} and i_{corr} value for different $Ti_{1-x}Al_xN$ thin films.

Transition metals and transition metal nitride coatings are in general relatively inert to the chemical attack as in the electrochemical series they are at relatively higher position. PVD techniques generally lead to porosity defects in the coatings during deposition and these pores act as primary source of corrosion. Film adhesion is another property influencing corrosion; in case of bad adhesion gas bubbles evolve during the corrosion study and result in fast degradation of the film [25, 26]. Thin film of TiAlN at higher power ratio shows good corrosion resistance due to the formation of denser microstructure. It reduced porosity observed at lower power ratio and was confirmed by the AFM image. There was negligible bubble formation during the corrosion test, it too supports that film obtained at higher power ratio is devoid of voids and resulted in films having good corrosion resistant. Film thickness of TiAlN coatings increased from 450 nm to 650 nm. Increase in film thickness results in reduction of corrosion behavior as suggested by Lang and Yu for TiN coating [27].

Du et al [18] showed that increased temperature in the absence of Al prevents the formation of α-Ti crystals which favors the formation of the TiN phase and considerably increases the hardness of the coatings. This confirms that when aluminum gets incorporated in excess to the coatings due to increased temperature at higher power ratio, the hardness of the coatings is improved. In our study, we found that at higher power ratio ternary phase appears which resulted in the formation of composite material having better properties.

4. CONCLUSION

The effect of RF/DC power ratio on the phase structure, microstructure, surface roughness and chemical composition of $Ti_{1-x}Al_xN$ coatings produced by co-sputtering have been investigated. Chemical compositions reveal that with increasing power ratios the Al/Ti ratio varied in the coating. The thickness of the coatings were found to be in the range 450 ~ 650nm. RMS roughness and the average roughness of the film surface decreases with increasing power ratio. SEM data showed that at higher power ratio surface morphology was smooth with smaller grain size in comparison to the films obtained at lower power ratio. XRD data reveal that with increase in RF/DC power ratio TiAlN (100) phase increases and TiAlN (114) phase decreases. Electrochemical experiments in 3.5% NaCl solution confirm that corrosion resistance of the TiAlN is better at higher RF/DC power ratio (DC power of 300W to Ti and RF power of 150W to Al targets).

6. REFERENCES
[1]. Munz W D, "Titanium aluminum nitride films: A new alternative to TiN coatings". J. Vac. Sci. Technol. 4 p 2717 (1986).
[2]. J.C. Oliveira, A. Manaia, A. Cavaleiro, "Hard amorphous Ti–Al–N coatings deposited by sputtering". Thin Solid Films 516 p 5032 (2008).
[3]. C. Chokwatvikul, S. Larpkiattaworn, S. Surinphong, C. Busabok, P. Termsuksawad, "Effect of Nitrogen Partial Pressure on Characteristic and Mechanical Properties of Hard Coating TiAlN Film". Journal of Metals, Materials and Minerals 21 p 115 (2011)
[4]. D.G. Park, T.H. Cha, S.H. Lee, I.S. Yeo, "Characteristics of sputtered $Ti_{1-x}Al_xN$ films for storage node electrode barriers". J. Vac. Sci. Technol. 19(6) p 2289 (2001).
[5]. J.T. Chen, J. Wang, F. Zhang, G.A. Zhang, X.Y. Fan, Z.G. Wu, P.X. Yan, "Characterization and temperature controlling property of TiAlN coatings deposited by reactive magnetron co-sputtering". J. Alloys compd. 472 p 91 (2009).
[6]. H. C. Barshilia, N. Selvakumar, K. S. Rajam, D. V. S. Rao, K. Muraleedharan, A. Biswas, "$TiAlN/TiAlON/Si_3N_4$ tandem absorber for high temperature solar selective applications". Appl. Phys. Lett. 89. 191909 (2006).
[7]. A. Biswas, D. Bhattacharyys, H.C. Barshilia, N. Selvakumar, K.S. Tajam, "Spectroscopic ellipsometric characterization of $TiAlN/TiAlON/Si_3N_4$ tandem absorber for solar selective applications". Appl. Surf. Sci. 254 p 1694 (2008).
[8]. H.C. Barshilia, N. Selvakumar, K.S. Rajam, A. Biswas, "Optical properties and thermal stability of TiAlN/AlON tandem absorber prepared by re active DC/RF magnetron sputtering". Sol. Energy Mater. Sol. Cells 92 p 1425 (2008).
[9]. B. Subramanian, R. Ananthakumar, M. Jayachandran, "Microstructural, mechanical and electrochemical corrosion properties of sputtered titanium-aluminum-nitride films for bio-implants". Vacuum 85 p 601 (2010).
[10]. J. Bujak, J. Walkowicz, J. Kusinski, "Influence of the nitrogen pressure on the structure and properties of (Ti,Al)N coatings deposited by cathodic vacuum arc PVD process". Surf. Coat. Technol. 180-181 p 150 (2004).
[11]. K. Chakrabarti, J.J. Jeong, S.K. Hwang, Y.C. Yoo, C.M. Lee, "Effects of nitrogen flow rates on the growth morphology of TiAlN films prepared by an rf-reactive sputtering technique". Thin Solid Films 406 p 159 (2002).
[12]. J.H. Hsieh, C. Liang, C.H. Yu, W. Wu, "Deposition and characterization of TiAlN and multi-layered TiN/TiAlN coatings using unbalanced magnetron sputtering". Surf. Coat. Technol. 108-109 p 132 (1998).
[13]. A. Shokrani, V. Dhokia, S.T. Newman, "Environmentally Conscious Machining of Difficult-to-Machine Materials with regards to Cutting Fluids". Int. J. Mach. Manuf. 57 p 83 (2012).
[14]. Caixian Tang, PhD thesis, Industrial Research Institute Swinburne (IRIS) Swinburne University of Technology Hawthorn, Victoria Australia (2007).
[15]. B.D. Beake, V.M.Vishnyakov, A.J.Harris, "Relationship between mechanical properties of thin nitride-based films and their behaviour in nano-scratch tests". Tribo. Inter. 44 p 468 (2011).
[16]. P.W. Shum, K.Y. Li, Z.F. Zhou, Y.G. Shen, "Structural and mechanical properties of titanium–aluminium–nitride films deposited by reactive close-field unbalanced magnetron sputtering". Surf. Coat. Technol. 185 p 245 (2004).
[17]. M.M. Hawkeye, M.J. Brett, "Glancing angle deposition: Fabrication, properties, and applications of micro- and nanostructured thin films". J. Vac. Sci. Technol. A 25 1317 (2007).
[18]. M. Du, L. Hao, X. Liu, L. Jiang, S. Wang, F. Lv, Z. Li, J. Mi, "Microstructure and thermal stability of $Ti_{1-x}Al_xN$ coatings deposited by reactive magnetron co-sputtering". Physics Procedia 18 p 222 (2011)
[19]. R. Messier, "Toward quantification of thin film morphology". J. Vac. Sci. Technol. A 4 p 490 (1986).

[20]. S. K. Mukherjee,a_ M. K. Sinha, B. Pathak, S. K. Rout, P. K. Barhai, "Anodic vacuum arc developed nanocrystalline Cu–Ni and Fe–Ni thin film thermocouples". J. Appl. Phys. 106 113717(2009).

[21]. H. Oettel, R. Wiedemann, "Residual stresses in PVD hard coatings". Surf. Coat. Technol. 76/77 p 265 (1995).

[22]. E.S. Gadelmawla, M.M. Koura, T.M.A. Maksoud, M. Elewa, H.H. Soliman, "Roughness parameters". J. Mat. Proc. Technol. 123 p 133 (2002).

[23]. A.Maksumov, R.Vidu, A.Palazoglu and P.Stroeve, "Enhanced feature analysis using wavelets for scanning probe microscopy images of surfaces". J. Colloid and Interface Science 272 p 365 (2004).

[24]. B. Subramanian, G. Umamaheswaru, M. Jayachandran, "Properties and corrosion behaviour of reactive magnetron sputtered TiAlN coatings on AISI 316L SS in simulated bodily fluid". Corr. Engg. Sci.Technol. 42 p 349 (2007).

[25]. H.W. Wang, M.M. Stack, S.B. Lyon, P. Hovsepian, W.D. Munz, "The corrosion behaviour of macroparticle defects in arc bond-sputtered CrN/NbN superlattice coatings". Surf. Coat. Technol. 126 p 279 (2000).

[26]. M. Fenker, M. Blazer, H.A. Jehn, H. Kappl, J.J. Lee, K.H. Lee, H.S. Park, "Improvement of the corrosion resistance of hard wear resistant coatings by intermediate plasma etching or multilayered structure". Surf. Coat.Technol. 150 p 101(2002).

[27]. F. Lang, Z. Yu, "The corrosion resistance and wear resistance of thick TiN coatings deposited by arc ion plating". Surf. Coat. Technol. 145 p 80(2001).